Electron-exchange collisions with molecular open-shell targets

I. Holtkötter[*] and G. F. Hanne[†]

Physikalisches Institut, University of Münster, Wilhelm-Klemm-Str. 10, 48149 Münster, Germany

(Received 23 June 2009; published 17 August 2009)

Low-energy electron-exchange collisions with the simple open-shell molecules O_2, NO, and NO_2 have been investigated by measuring the change in electron-spin polarization after scattering polarized electrons from unpolarized molecules with energies between 8 and 20 eV and scattering angles up to 130°. Results for elastic collisions with O_2 and NO are compared with existing theories where the agreement is fair. Direct observation of spin-exchange collisions is obtained for elastic scattering from NO_2 and for electron-impact excitation of O_2 (6.1 eV energy loss). It is also shown that the results may be influenced by spin-orbit interaction, which was assumed to be negligible in previous studies.

PACS number(s): 34.80.Nz

I. INTRODUCTION

Low-energy electron collisions with simple open-shell molecules such as O_2, NO, or NO_2 play an important role in both atmospheric physics and plasma chemistry. Elastic and inelastic electron scatterings at low energies are expected to be significantly influenced by exchange processes in which the incoming electron and a bound electron change places.

Exchange processes can be made visible if the spin projections of the two electrons involved have opposite directions. The spin can then be used as a marker to distinguish between the two electrons. Such exchange processes reduce the spin polarization of the scattered electron beam and are therefore measurable by means of a spin analysis of the incoming and the scattered electron beams. However, the spin-orbit interaction may also lead to similar effects and thus these investigations should be carried out with low-Z targets and/or small scattering angles, where spin-orbit effects are small.

To investigate elastic exchange processes, one must use paramagnetic targets with unsaturated spin configuration, because only these can lead to observable "spin flips" by exchange of electrons with opposite spin directions. Of course, exchange between electrons with parallel spin orientations occurs in these targets as well, which would not lead to spin flips. On the other hand, exchange with electrons from spin-saturated targets can take place only between electrons with the same spin projection and thus cannot be observed directly.

Electron-exchange collisions with paramagnetic atoms and molecules such as Na, Hg, O_2, or NO have been studied previously [1]. Whereas the agreement of experimental and theoretical results is, in general, very good for the atomic targets, discrepancies between the measurements and the theoretical data of the Schwinger multichannel method used by da Paixão *et al.* [2], of the Schwinger distorted-wave approximation (DWA) method by Machado *et al.* [3], and of the R-matrix calculations calculated by Nordbeck *et al.* [4] and Wöste *et al.* [5] must be noted for molecular targets.

Hence, we modified these measurements with a higher accuracy to take a closer view at these discrepancies. In the present work a number of experimental data showing the significance of exchange collisions of spin-polarized electrons with oxygen molecules, nitrogen monoxide, and nitrogen dioxide [6] are presented and compared with previous [2–5] and recent [7,8] theoretical calculations.

II. THEORETICAL BACKGROUND

The formal analysis of scattering processes of spin-polarized electrons with unpolarized molecules can be done in the collision frame, in which the incident electron beam defines the z axis. The directions of the incident and the outgoing electrons span the zx scattering plane. In Fig. 1 all the important scattering parameters are defined: an incoming electron beam with the wave vector $\vec{k}$ and the polarization vector $\vec{P}$ hits a molecule (shown without further structure) in the scattering center. The scattered outgoing electrons can be observed with the wave vector $\vec{k}'$ and the polarization vector $\vec{P}'$ after scattering.

Due to the mixed states given in the experiment, it is useful to apply the density-matrix formalism to describe the scattering reaction. According to theoretical investigations [9], we can parametrize the reduced density matrix of the final state with eight real parameters if we observe the outgoing electrons only. These parameters can be identified by the differential cross section σ_u for scattering with unpolar-
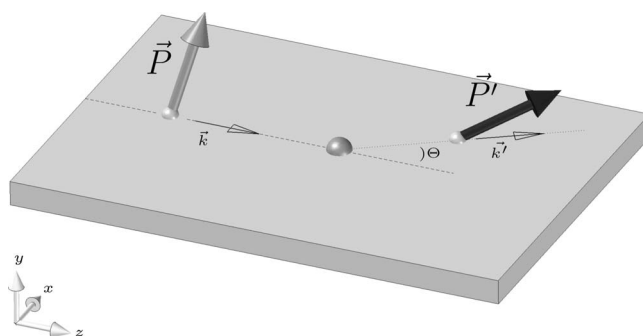

FIG. 1. Scheme of the scattering plane.

*ingo.holtkoetter@uni-muenster.de

†hanne@uni-muenster.de

ized electrons and seven generalized S, T, U parameters, which describe the transition from the initial polarization $\vec{P}$ to the final polarization $\vec{P}'$ after the scattering process,

$$\sigma(\Theta) = \text{tr}\{\rho_J\} = \sigma_u(\Theta)(1 + P_y S_A), \tag{1}$$

$$\vec{P}' = \frac{\text{tr}\{\rho_J \tilde{\sigma}\}}{\text{tr}\{\rho_J\}} = \frac{1}{1 + P_y S_A} \begin{pmatrix} T_x P_x + U_{xz} P_z \\ T_y P_y + S_P \\ T_z P_z - U_{zx} P_x \end{pmatrix}. \tag{2}$$

Here, $\sigma(\Theta)$ is the cross section for polarized electrons. The three contraction parameters T_x, T_y, and T_z describe the three-dimensional compression of the polarization vector; U_{xz} and U_{zx} describe a rotation in the scattering plane from z in the x direction (U_{xz}) and from x in the z direction (U_{zx}), respectively; and S_A and S_P describe the asymmetry and the polarization function, respectively. Note that, for elastic collisions, $S_A = S_P = S$ is the so-called Sherman function.

If we consider the polarization components perpendicular to the scattering plane only, the expression for the outgoing polarization reduces to

$$P_y' = \frac{1}{1 + P_y S_A}(T_y P_y + S_P). \tag{3}$$

We can assign cross-section fractions ($\sigma_{in,out}$), where the arrows describe the possible spin components of the incoming and the outgoing electrons perpendicular to the scattering plane, to the parameters in Eqs. (1) and (3) by

$$\sigma_u = \tfrac{1}{2}[\sigma_{\uparrow\uparrow} + \sigma_{\uparrow\downarrow} + \sigma_{\downarrow\uparrow} + \sigma_{\downarrow\downarrow}], \tag{4}$$

$$S_P = \tfrac{1}{2}[\sigma_{\uparrow\uparrow} + \sigma_{\uparrow\downarrow} - \sigma_{\downarrow\uparrow} - \sigma_{\downarrow\downarrow}]/\sigma_u, \tag{5}$$

$$S_A = \tfrac{1}{2}[\sigma_{\uparrow\uparrow} - \sigma_{\uparrow\downarrow} + \sigma_{\downarrow\uparrow} - \sigma_{\downarrow\downarrow}]/\sigma_u, \tag{6}$$

$$T_y = \tfrac{1}{2}[\sigma_{\uparrow\uparrow} - \sigma_{\uparrow\downarrow} - \sigma_{\downarrow\uparrow} + \sigma_{\downarrow\downarrow}]/\sigma_u. \tag{7}$$

In Eq. (7) it can easily be seen that the T_y parameter is a direct measure for spin-flip processes. If the spin-orbit interaction is negligible, we have $S_P = S_A = 0$, meaning $\sigma_{\uparrow\uparrow} = \sigma_{\downarrow\downarrow}$ and $\sigma_{\uparrow\downarrow} = \sigma_{\downarrow\uparrow}$. In that case the T_y parameter is influenced by exchange collisions only and can be determined by measuring the incoming and the outgoing spin-polarization components perpendicular to the scattering plane [cf. Eq. (3) with $S_A = S_P = 0$],

$$\frac{P_y'}{P_y} = T_y. \tag{8}$$

Finally, the T_y parameter can be transformed into the spin-flip probability w_{SF} by combining Eqs. (4) and (7) as follows:

$$T_y = 1 - 2w_{\text{SF}}, \quad w_{\text{SF}} = \tfrac{1}{2}[\sigma_{\uparrow\downarrow} + \sigma_{\downarrow\uparrow}]/\sigma_u. \tag{9}$$

The description of the parameter T_y in terms of scattering amplitudes can be found elsewhere [1]. We note that the oxygen molecule with the ground-state configuration $^3\Sigma_g^-$ is a spin-1 target whereas NO ($^2\Pi$) and NO_2 ($^2A_1$) are spin-1/2 targets.
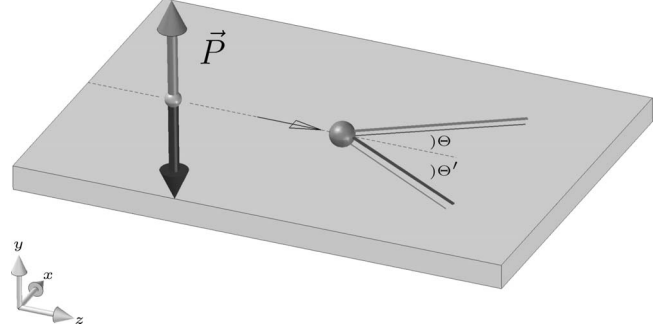

FIG. 2. Scheme of a S_A measurement.

III. SCATTERING PARAMETER MEASUREMENTS

A. Exchange parameter T_y

According to Eq. (8) two polarization measurements are needed to determine the exchange parameter T_y. For the primary polarization measurement P_y, the electron analyzer is set to 0° position and the electron beam is guided into the Mott analyzer directly. After that, the electron analyzer is moved to the scattering angle of interest and the polarization of the scattered electron beam P_y' is measured. Before and after the polarization measurements, our measurement cycle involves angular calibration measurements to check the shape and the alignment of the electron beam.

B. Asymmetry parameter S_A

To investigate the asymmetry parameter S_A [see Eq. (1)], one has to measure the intensity of the scattered electron beam with respect to the incident spin polarization (see Fig. 2). The obtained spin-up or -down asymmetry is a direct measure for the parameter S_A,

$$S_A = \frac{1}{P_y}\left(\frac{N(\uparrow) - N(\downarrow)}{N(\uparrow) + N(\downarrow)}\right). \tag{10}$$

In order to eliminate instrumental asymmetries, we carried out the measurements with positive and negative scattering angles and calculated the corrected asymmetry parameter (ideal case: $S_A^+ = -S_A^-$),

$$S_A = \frac{S_A^+ - S_A^-}{2}. \tag{11}$$

If the parameters S_A and S_P are different from zero and cannot be neglected, the exchange parameter T_y has to be recalculated. With Eq. (3) we get instead of Eq. (8)

$$T_y = \frac{P_y'(1 + P_y S_A) - S_P}{P_y}. \tag{12}$$

Even if S_A and S_P have very small values, they may have a significant influence on the T_y parameter, which can be seen within the accuracy we achieved in our measurements (see results for nitrogen dioxide).
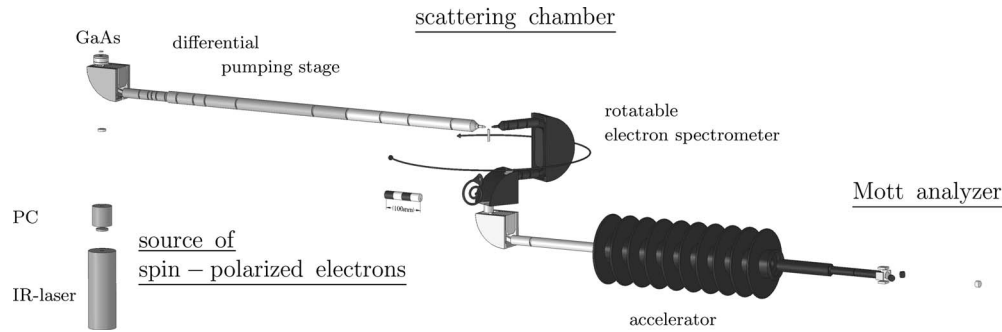
FIG. 3. Experimental apparatus overview: on the left, one can see the source of polarized electrons with IR laser, Pockels cell, 90° deflector, and GaAs crystal. The electron is focused through a differential pumping stage into the scattering region where it hits the target. The scattered electrons are analyzed by a rotatable electron spectrometer and then guided into the Mott analyzer to determine the spin polarization.

C. Experimental apparatus

This section contains a short overview of the experimental apparatus used for these investigations (see Fig. 3 for a schematic of the experiment).

1. Source of polarized electrons

The use of spin-polarized photoelectrons extracted from a GaAs crystal by irradiation of a circular polarized infrared laser beam is a common method for spin-polarized electron sources (e.g., see [1,10]). Hence, we report only the typical operating conditions of our source (see Table I).

2. Targets

The gas targets were fed from gas cylinders through a leak valve system into the scattering chamber where a metal-shielded glass microchannel array (length of 1 mm and channel diameter of 10 μm) in the scattering region led to a well-defined and collimated gas jet. In order to establish a background correction, a remote-controlled valve directed the gas jet either into the scattering region or to a bypass leak. The experimental results were obtained by measuring the difference in count rates between the scattering region and the bypass gas jet.

The gas cylinders were supplied by Air Liquide with purities of 99.998% (O_2), 99.5% (NO), and >99% (NO_2). In the case of NO_2 one has to take into account that, at room temperature, NO_2 and its dimer $(NO_2)_2$ are both present in the gas jet. To minimize the $(NO_2)_2$ fraction, the gas capillary and the nozzle in the scattering recipient were heated to 130 °C to reduce the fraction of $(NO_2)_2$ to far below 1%. Additional water impurities in the gas cylinder were frozen out with a cooling trap at −10 °C between the gas cylinder and the leak valve system.

3. Scattering chamber and Mott detector

The scattered electrons from the scattering region pass through a 180° energy analyzer, which is rotatable in the scattering plane. A twofold 90° deflection unit guides the analyzed electrons toward the Mott detector after acceleration to 120 keV to determine the spin polarization of the electron beam. This setup allows us to measure at scattering angles between −138° and +142° (see Table I for important experimental parameters).

In order to compare our experimental results with other data, we made several test measurements to calibrate our apparatus. For energy calibration, photons were observed from electron-impact ionization of xenon atoms at a scattering energy of 10.97 eV with a photomultiplier to determine the optical excitation function ($7p[2\frac{1}{2}]_3 \rightarrow 6s[1\frac{1}{2}]_2$). The con-

TABLE I. Important parameters of the experimental apparatus.

Source of spin-polarized electrons
Chamber pressure: $<3 \times 10^{-11}$ hPa
Laser wavelength: 808 nm
Emission current: $2-4$ μA typ.
Beam lifetime chamber closed: >4 weeks
Beam lifetime during measurement: 24 h (O_2),
96 h (NO, NO_2) (multiple Cs evaporations possible)
Electron beam polarization: $27-30$ %
Preparation lifetime: >12 months

Scattering chamber
Pressure chamber closed: $<3 \times 10^{-7}$ hPa
Chamber pressure during measurement: $(2-5) \times 10^{-6}$ hPa
Angular range for detection system: $-138°-+142°$
Beam current in the scattering center: 50–450 nA
Typ. overall angular resolution at 10 eV: $\pm 3°-5°$
Typ. overall energetic resolution at 10 eV: ± 600 meV

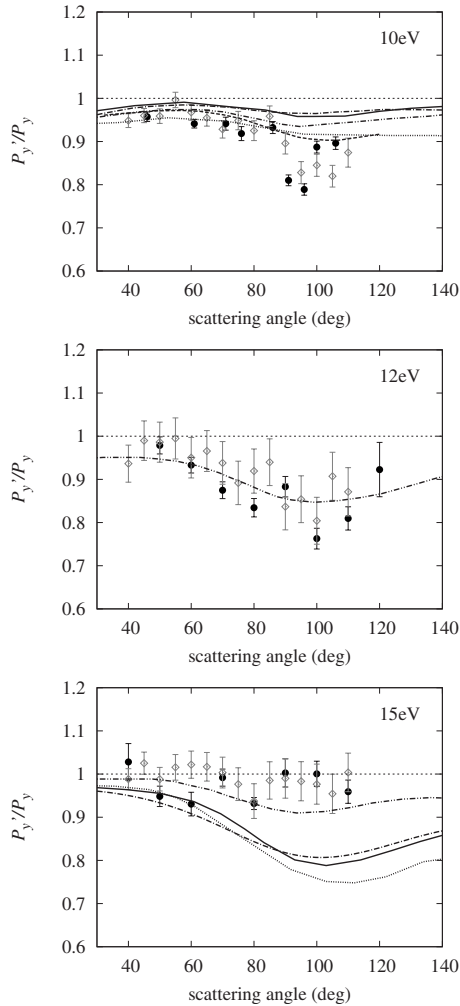| Mott detector |
| --- |
| Chamber pressure: $<1 \times 10^{-6}$ hPa |
| S_{eff}: −0.24 (110 nm foil) |
| Scattering energy: 120 keV |
| Dark counts per detector: 1–10 counts/m |
| Count rates: 1000–3000 counts/s (P_0 measurement) |
| 10–100 counts/s (typ. T_y measurement) |

FIG. 4. Exchange parameter O_2 at 10, 12, and 15 eV. Experiment: present results (●) and Hegemann *et al.* [12] (◇); calculations: Nordbeck *et al.* [4] (—), da Paixão *et al.* [2] (·····), Wöste *et al.* [5] (– –), Machado *et al.* [3] (–·–·), and Tashiro [7] (–··–··).

FIG. 5. Exchange parameter O_2 at 100°. Experiment: present results (●), Hegemann *et al.* [11] (◇), and Schroll [13] (□); calculations: Fullerton *et al.* [14] (—), Wöste *et al.* [5] (– –), and Tashiro [7] (–··–··).

rameter P_y'/P_y with randomly oriented O_2 molecules at electron-impact energies of 10, 12, and 15 eV together with the previous measurements of Hegemann *et al.* [12] and theoretical data of da Paixão *et al.* [2], Nordbeck *et al.* [4], Wöste *et al.* [5], Machado *et al.* [3], and Tashiro [7].

For their calculations, da Paixão *et al.* used a three-state Schwinger multichannel variational principle, Machado *et al.* used a combined Schwinger variational iterative method (SVIM) and distorted-wave approximation (DWA) method, Tashiro used a 13-state *R*-matrix calculation, Nordbeck *et al.* used a nine-state *R*-matrix calculation, and Wöste *et al.* extended the method of Nordbeck *et al.* method with a special emphasis on vibrational excitations. Wöste *et al.* used two vibrationally averaged symmetries ($^4\Sigma_u^-$ and $^2\Sigma_u^-$) and ten fixed nuclei symmetries instead of fixed nuclei T matrices for all 12 scattering symmetries. One can still see noticeable discrepancies between the theoretical and the previous and the present experimental data for 10 and 15 eV, whereas the agreement at 12 eV is satisfactory.

To shed light on this findings, experimental data for the polarization fraction at a fixed angle of 100° with energies between 8 and 15 eV are shown in Fig. 5 together with previous experimental results of Schroll [13] and theoretical *R*—matrix calculations of Fullerton et al. [13]. We note that the different theories differ considerably from each other in shape and magnitude where the recent *R*-matrix calculation [7] shows the best agreement with the experimental data.

B. Inelastic collisions from O_2 molecules

Figure 6 shows measurements of the polarization fraction of inelastically scattered electrons from the oxygen molecule. These measurements are very difficult due to the approximately 100 times smaller differential cross sections of the inelastic transition and require much longer accumulation times in comparison with the elastic-scattering processes. For this reason we chose small scattering angles for our measurements to achieve higher count rates. At an energy loss of 6.1 eV, the excitation may be dominated by the triplet-singlet part of the transition into the 6.1 eV region [$X\,^3\Sigma_g^- \rightarrow (c\,^1\Sigma_g^-$, $C\,^3\Delta_u$, and $A\,^3\Sigma_u^+)$] [15]. For a pure triplet-singlet transition, a ratio $P_y'/P_y = -1/3$ would be expected. Indeed, because of the large deviations from $P_y'/P_y = 1$, the observed exchange

tact potential between the GaAs crystal and the scattering center was between 3.5 and 3.7 eV. This measurement was repeated regularly to assure correct scattering energy values for comparison with other data.

During our measurements of the exchange parameter, the angular position and the shape of the electron beam were measured by moving the electron spectrometer through an angular range of −10° to +10°. Thus, an accidental influence of misalignment or drifts in angular position of the electron beam on the experimental results could be avoided.

To determine the spin polarization of the electron beam, we used a conventional high-energy Mott detector with monitor counters. Great care was taken to avoid misalignment and false asymmetries caused by the rotation of the electron spectrometer during the measurements.

IV. RESULTS

A. Elastic collisions from O_2 molecules
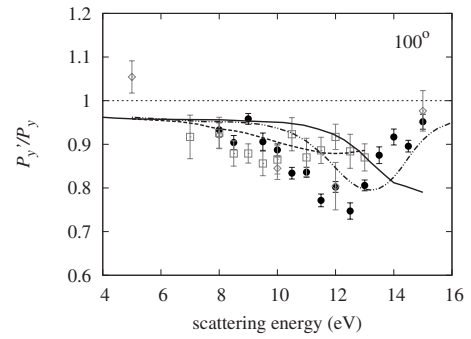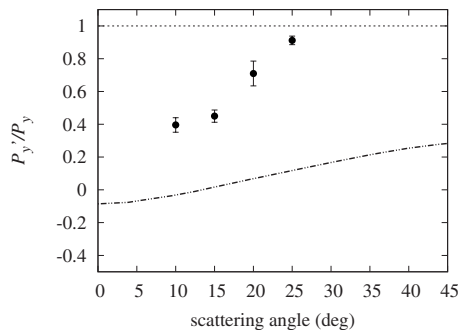
Figure 4 presents our recent results for the exchange pa-

FIG. 6. Exchange parameter O_2 at 18 eV scattering energy and 6.1 eV energy loss. Present results ($\bullet$); calculation [$X\,^3\Sigma_g^- \to$ ($c\,^1\Sigma_u^-$, $C\,^3\Delta_u$, and $A\,^3\Sigma_u^+$)]: Tashiro ($-\cdot\cdot-\cdot\cdot$) [8].

effects seem to be strongly influenced by the triplet-singlet transition.

C. Elastic collisions from NO molecules

Figure 7 shows our results for the exchange parameter for elastic electron scattering with NO at 8 and 10 eV. For the experimental data in the case of 10 eV, we achieve a fair agreement with the theoretical data. Figure 8 extends these measurements to the energy range between 8 and 15 eV at a fixed angle of 80°. New calculations of this scattering system are desirable.

D. Elastic collisions from NO$_2$ molecules

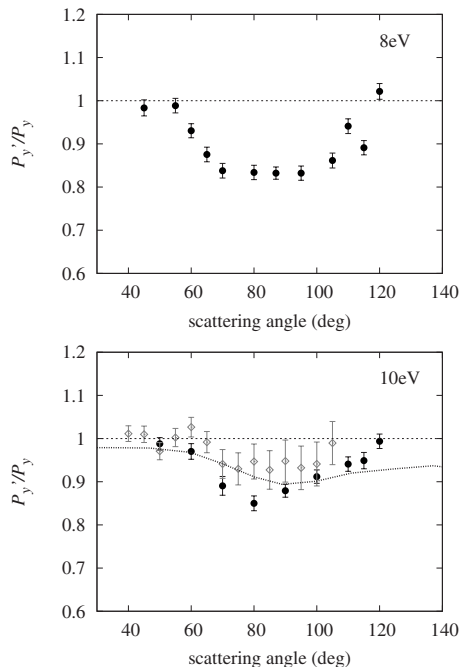For NO$_2$, no experimental and theoretical data for spin-exchange effects were available. In comparison to the linear

FIG. 7. Exchange parameter NO at 8 and 10 eV. Experiment: present results ($\bullet$) and Hegemann *et al.* [11] ($\diamond$); calculations: da Paixão *et al.* [2] ($\cdots\cdots$).

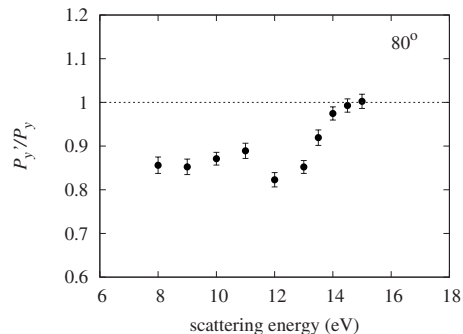

FIG. 8. Exchange parameter NO at 80°: present results ($\bullet$).

diatomic molecules O_2 and NO, the theoretical description of the triatomic bent NO$_2$ molecule is more complicated. The additional degrees of freedom due to intermolecular angle and internuclear distances lead to a complex energetic structure, so that the energetic levels of this molecule are not well known and are still under investigation [16].

In Fig. 9 results for elastic collisions at 8 and 12 eV are shown. Whereas for 8 eV significant exchange effects are visible at angles about 60° and 115°, the measurements at 12 eV result in several values of $P_y'/P_y > 1$ (see Fig. 9, black dots). Values of $P_y'/P_y > 1$ cannot be the result of exchange collisions only. Therefore, we decided to investigate the influence of the Sherman function on the exchange parameter. We found out that even with light targets such as NO$_2$, the Sherman function has a strong influence on the polarization fraction P_y'/P_y if the incident polarization P_y is as low as 0.3 and only small spin-exchange effects are present. In such a case even small values of the Sherman function have a significant influence on the exchange parameter and we have to use Eq. (12) to obtain the correct T_y parameter. For elastic
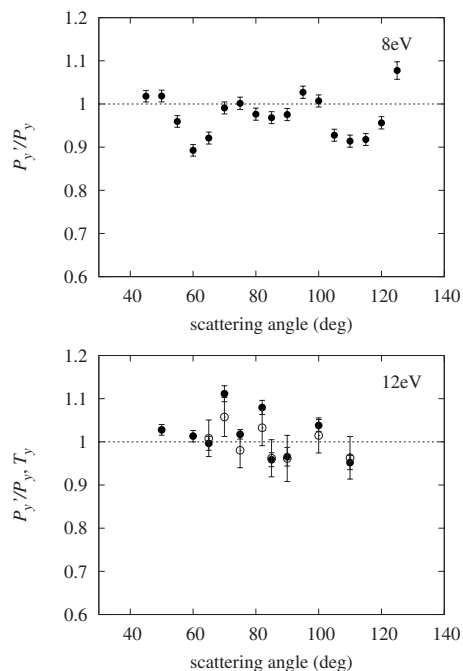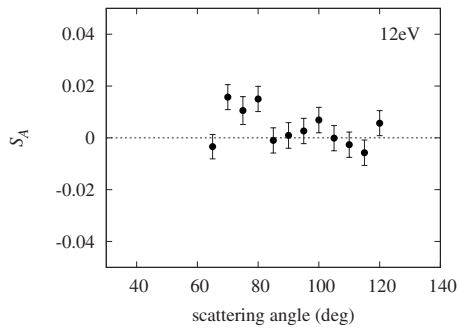

FIG. 9. Exchange parameter NO$_2$ at 8 and 12 eV: P_y'/P_y ($\bullet$) and T_y results ($\circ$) corrected with S_A values.

FIG. 10. S_A-parameter NO_2 at 12 eV: present results (●).

scattering we can assume $S_A = S_P = S$. Figure 9 shows the P_y'/P_y measurement and the T_y parameter, which has been corrected by the use of the corresponding S_A values (see Fig. 10). As one can see, the probability of electron-exchange scattering with NO_2 is very small: no clear deviation of $T_y = 1$ is visible after correction. In future experimental and theoretical investigations, it seems to be important to include the influence of the Sherman function for elastic electron scattering at low energies. Another series of measurements at a fixed scattering angle of 110° at scattering energies between 8 and 15 eV is presented in Fig. 11.

V. CONCLUSIONS

A number of experimental results for low-energy electron-exchange collisions with the simple open-shell molecules O_2, NO, and NO_2 have been presented and are available for comparison with theoretical calculations. In general, the effects
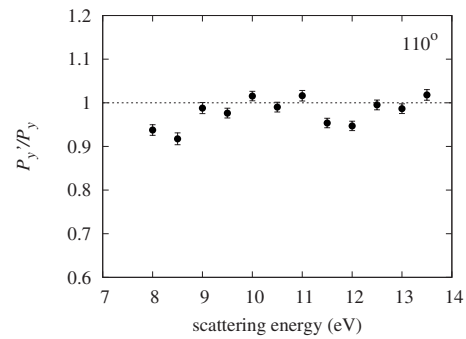
FIG. 11. Exchange parameter NO_2 at 110°: present results (●).

are small compared to scattering with, e.g., alkali-metal atoms. In the case of O_2 the experimental results show stronger exchange effects at a scattering angle of 100° and energies of about 12 eV. For NO the effects are stronger at 8 eV. As expected in comparison to direct scattering, the exchange is more dominant in electron-impact excitation of the 6.1 eV peak in O_2, where a triplet-singlet transition is likely to dominate the process. For the triatomic paramagnetic molecule NO_2, we present experimental results, but so far there are no calculations available for this target. As demonstrated in the case of NO_2, we cannot neglect the Sherman function even for low-Z targets to determine the T_y parameter if spin-exchange effects are small. The R-matrix calculation by Tashiro [7] for collisions with O_2 is obviously a theoretical progress; however, more theoretical data for the other targets are desirable to achieve a better understanding of spin-exchange processes in electron scattering with simple paramagnetic molecules.

[1] T. Hegemann, Ph.D. thesis, University of Münster, 1992.

[2] F. J. da Paixão, M. A. P. Lima, and V. McKoy, Phys. Rev. Lett. **68**, 1698 (1992).

[3] L. E. Machado, E. M. S. Ribeiro, M.-T. Lee, M. M. Fujimoto, and L. M. Brescansin, Phys. Rev. A **60**, 1199 (1999).

[4] R.-P. Nordbeck, C. M. Fullerton, G. Woeste, D. G. Thompson, and K. Blum, J. Phys. B **27**, 5375 (1994).

[5] G. Wöste, K. Higgins, P. Duddy, C. M. Fullerton, and D. G. Thompson, J. Phys. B **29**, 2553 (1996).

[6] I. Holtkötter, Ph.D. thesis, University of Münster, 2008.

[7] M. Tashiro, Phys. Rev. A **77**, 012723 (2008).

[8] M. Tashiro (private communication).

[9] K. Bartschat, Phys. Rep. **180**, 1 (1989).

[10] D. T. Pierce, R. J. Celotta, G.-C. Wang, W. N. Unertl, A. Galejs, C. E. Kuyatt, and S. R. Mielczarek, Rev. Sci. Instrum. **51**, 478 (1980).

[11] T. Hegemann, M. Oberste-Vorth, R. Vogts, and G. F. Hanne, Phys. Rev. Lett. **66**, 2968 (1991).

[12] T. Hegemann, S. Schroll, and G. F. Hanne, J. Phys. B **26**, 4607 (1993).

[13] S. Schroll, Master's thesis, University of Münster, 1992.

[14] C. M. Fullerton, G. Woeste, D. G. Thompson, K. Blum, and C. J. Noble, J. Phys. B **27**, 185 (1994).

[15] K. Wakiya, J. Phys. B **11**, 3931 (1978).

[16] P. P. Bera, Y. Yamaguchi, and H. F. Schaefer, J. Chem. Phys. **127**, 174303 (2007).